All responses will be presented in Times New Roman font. The responses will appear in black, while revisions made to the manuscript will be highlighted in blue.

Reviewer 2

Summary

This study explores HOM formation via the H-abstraction pathway of alpha-pinene OH-oxidation by conducting photo-oxidation experiments of alpha-pinene and pinonaldehyde in the SAPHIR-STAR chamber at varying NO levels using H2O2 as an oxidant precursor. This work is novel as it explores another possible source for H-abstraction HOM-RO2 and subsequent products (i.e. pinonaldehyde OH-oxidation). Using two types of chemical ionization techniques and fuzzy c-means clustering, this study finds that fractional contribution of H-abstraction HOM-RO2 and subsequent termination products to total HOM increased with increasing NO.

It's my determination that this work is both within the scope of this journal and the results from these experiments can prove beneficial to the field. However, I have some concerns about the analysis of the data, and I believe some deeper analysis could increase the novelty of the work. Therefore, I recommend reconsidering this manuscript after major revisions.

Major comments

1. *Regarding the experimental setup, a focus is placed on the no NO case having no NO. However, is there no NO or is the level of NO below the limit of detection of your instrument? No LOD is given, and, as shown in the Shen 2022 paper, an off-gassing of HONO from chamber walls could delay a NO reaction with the initial H-abstraction RO2 (C10H15O2) resulting in a delay of isomerization and subsequent HOM-RO2 formation. I have a similar comment with the O3 measurement. What is the LOD and what is the O3 production during the "early reaction stage" (this can be estimated with some 0D box modeling, see below)?*

Responses:

We thank the reviewer for his thoughtful review of our manuscript and for this comment. We agree that the detection limits of NO and O_3 are particularly important, especially in the early reaction stages. The detection limits of NO and O_3 are 0.05 ppb and 0.2 ppb, respectively. Additionally, it should be mentioned that the chamber used in this study is made from glass (Baker et al., 2024) and will not outgas HONO.

These detection limits do not affect our definition of early reaction stage periods, or the subsequent analysis. For example, during the early reaction stages, O_3 production was generally less than 1 ppbv. Therefore, the loss of α-pinene via O_3 oxidation was negligible compared to OH oxidation. We have now added information about the limits of detection to the instrumentation section.

Gas concentrations of NO and NO_x were detected by a NO monitor (nCLD 899, Eco Physics GmbH) coupled to a self-built photolytic NO_2 converter, with a detection limit of 0.05 ppb for NO measurement. The O_3 was measured by an O_3 monitor (O342e, Envea GmbH), with a detection limit of 0.2 ppb.

2. The authors discussion identifying the "early reaction stage" is unclear to me since the reasoning is not quantitative. This could be limiting their analysis by comparing across the experiments at different extents of reaction. Because they measure many key compounds that affect RO2 and VOC fate, such as NO, HO2, OH, and O3, I recommend some RO2 parameterization and reaction modeling be included in this study to enhance their discussion of RO2 fate and FCM analysis by quantifying the "early reaction stage".

Responses:

We also thank the reviewer for the suggestion to use box model simulations to estimate the concentrations of RO_2·, HO_2·, and ·OH, thereby providing a more quantitative definition of the early reaction stage period. Accordingly, we have performed additional box model simulations for the α-pinene photooxidation experiments, with the chemical mechanistic information based on the Master Chemical Mechanism, MCM v3.3.1 (Jenkin et al., 1997; Saunders et al., 2003). The results were added to Section 2.2: "Model Simulations to Determine Early Reaction Stages" of the manuscript. The relevant diagrams are shown now in Figure 2.

Based on the results of these simulations, the early reaction stage periods are now identified by the RO_2· fate and the loss of α-pinene and pinonaldehyde. In summary, we define the early reaction stages by using three criteria: (i) α-pinene turnover exceeds that of pinonaldehyde by a factor of ten, (ii) under conditions with NO, biomolecular reactions of RO_2· are dominated by RO_2· + NO, contributing more than 90% to RO_2· biomolecular losses, (iii) α-pinene oxidation is primarily driven by ·OH rather than O_3.

However, the determination of early reaction stages by using these box model simulations does not show significant change because previously we had already considered the influence of the RO_2 fate, O_3 reactions, and pinonaldehyde by using less refined model simulations. Previously, early reaction stages were identified within 100 seconds, 100 seconds, and 300 seconds for NO-free, low-NO, and high-NO conditions, respectively. The updated version only changes the length of the period for high-NO conditions to 320 seconds, while time periods for NO-free and low-NO conditions stay the same with 100 seconds.

The newly added Section 2.2: "Model Simulations to Determine Early Reaction Stages" and the updated and added figures in the manuscript and the supplemental material are shown below:

Model simulations to determine early reaction stages

To clarify the role of the H-abstraction channel under varying NO conditions the early reaction stages are particularly relevant. In this study, we define early reaction stages using three criteria: (i) α-pinene turnover exceeds that of pinonaldehyde by a factor of ten, (ii) under conditions with NO, biomolecular reactions of RO_2· are dominated by RO_2· + NO and contribute more than 90% to the biomolecular loss of RO_2·, and (iii)

α-pinene oxidation is primarily driven by ·OH rather than O_3. Therefore, model simulations for α-pinene photooxidation systems were conducted to quantitively identify these early reaction stages.

As shown in ***Figure 2 (a-1) to (c-1)***, the model captures the evolution of the system quite well but generally underestimates NO and O_3 concentrations. These discrepancies may arise from differences in the temporal resolution of measurements and simulations, physical effects introduced by the activation of the UVC lamps (e.g., changing emissions due to temperature adjustment of the UVC lamp), and uncertainties in the chemical mechanism including reactions currently not represented in the model framework. The HO_2· and RO_2· concentrations obtained from the simulations are shown in ***Figure 2 (a-2) to (c-2)*** together with the relative contributions of RO_2· + NO, RO_2· + HO_2· and RO_2· + NO to the total biomolecular RO_2 loss. Here, the reaction rates were calculated with $k_{[RO2][HO2]} = 1.85 \cdot 10^{-11}$ cm^3 s^{-1}, $k_{[RO2][NO]} = 1 \cdot 10^{-11}$ cm^3 s^{-1} and $k_{[RO2][RO2]} = 5 \cdot 10^{-12}$ cm^3 s^{-1} (Baker et al., 2024; Berndt et al., 2016; Jenkin et al., 1997).

Based on these results, reactions occurring within the first 100 s, 100 s, and 320 s after initiation of reactions by starting the photooxidation were defined as early stages for the NO-free, low-NO, and high-NO conditions, respectively. The average bimolecular reaction rates for RO_2· + NO were negligible for cases without NO and increased to 0.179 s^{-1} and 1.06 s^{-1} for the low-NO and high-NO conditions, respectively. For RO_2· + HO_2· reactions, the rates were 0.0055 s^{-1}, 0.011 s^{-1}, and 0.0075 s^{-1}, while those for RO_2· + RO_2· reactions were 0.0075 s^{-1}, 0.0029 s^{-1}, and 0.0014 s^{-1} for NO-free, low-NO, and high-NO conditions, respectively. The contribution of RO_2· + NO was higher than 90% under both low-NO and high-NO conditions.

For pinonaldehyde photooxidation under high-NO conditions, the reactions within the early reaction stages were also investigated to facilitate comparison with the corresponding α-pinene system under high NO conditions. Besides H-abstraction channel, reactions of α-pinene with O_3, and pinonaldehyde with ·OH may also contribute to the formation of $C_{10}H_{15}O_x$ radicals. Therefore, the loss of α-pinene due to oxidation by O_3 formed as a byproduct of other reactions, and the loss of pinonaldehyde via ·OH oxidation, were evaluated. The results are shown in detail in ***Figure S7***. In both cases, losses are smaller than 1% of the reaction rate of α-pinene with ·OH, which further supports our definition of early reaction stage being reasonable and representative.

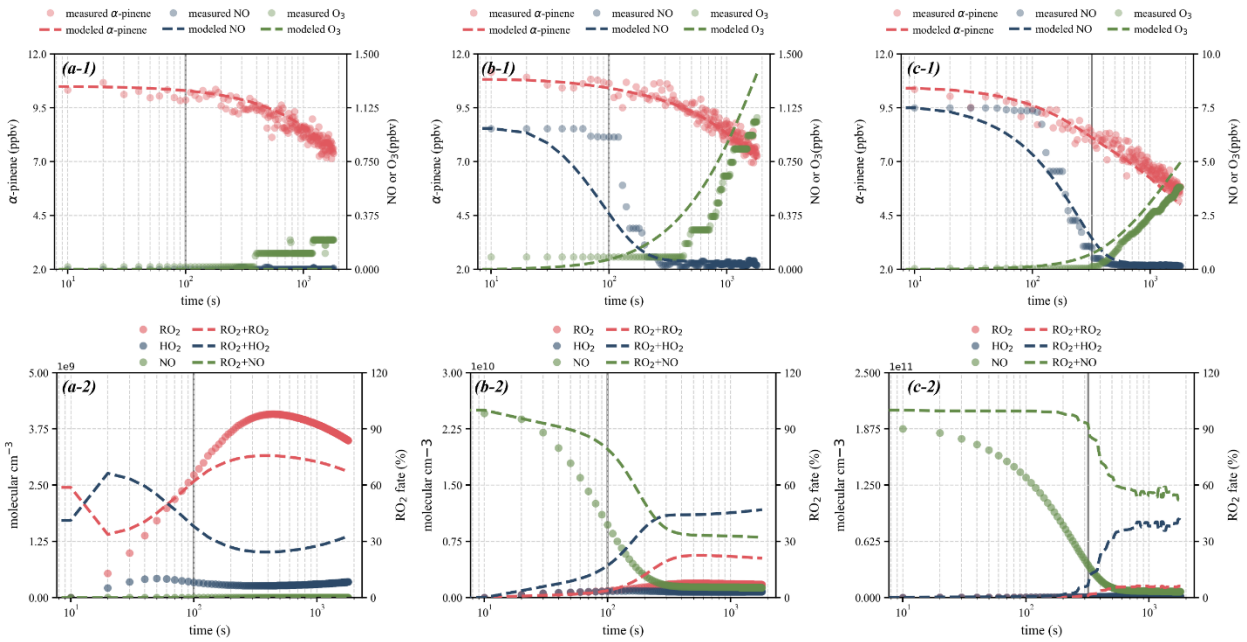

Figure 2. Results of model simulations for α-pinene photooxidation under NO-free (a-1, a-2), low-NO (b-1, b-2), and high-NO conditions (c-1, c-2). The upper panels show modeled and measured concentrations of α-pinene, NO, and O_3 across the three conditions, while the lower panels show the corresponding radical concentrations of RO_2· and HO_2·. In addition, the lower panels illustrate the relative contributions of RO_2· + HO_2·, RO_2· + RO_2· and RO_2· + NO reactions to the total bimolecular reaction rate of RO_2· (shown as RO_2· fate on the right y-axis).

Figure S7 was added to the supplemental information:

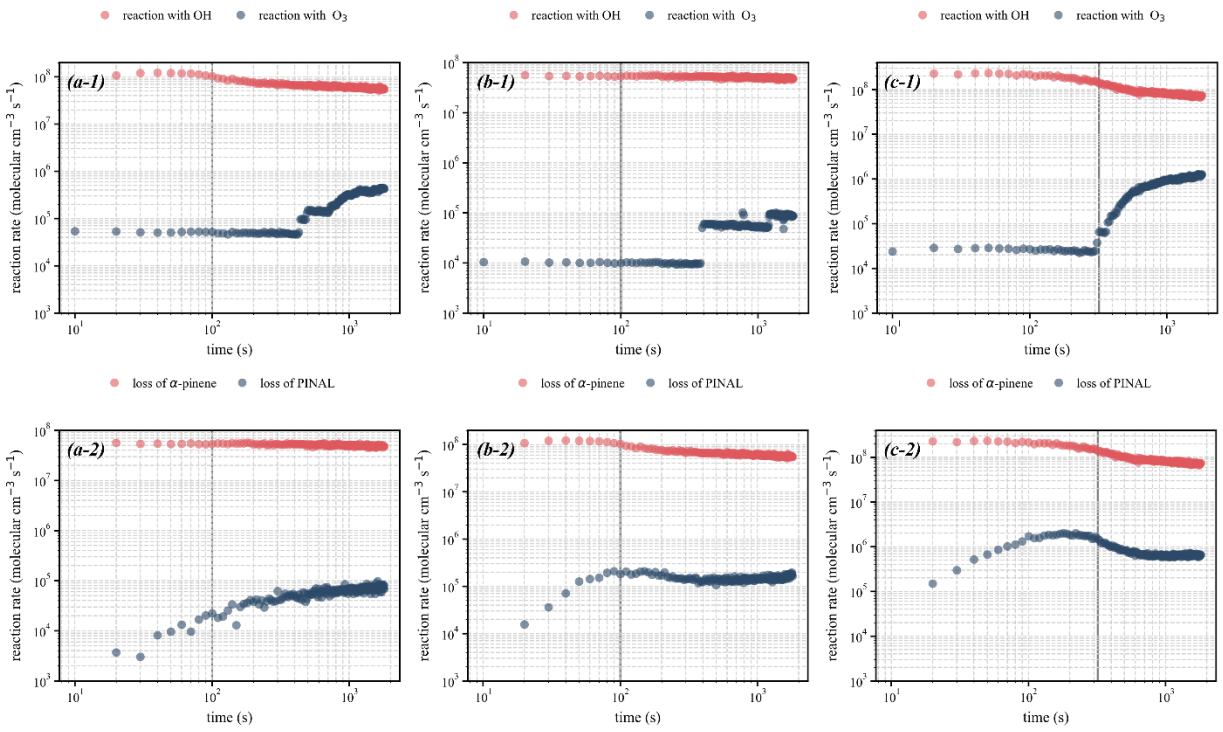

Figure S7. The upper panels (a-1 to c-1) compare the oxidation rates of α-pinene by ·OH and O_3 under NO-free, low-NO, and high-NO conditions, respectively. In each case, the relative contributions of OH- and O_3-initiated oxidation are shown. The lower panels (b-1 to c-1) compare the OH-initiated reaction losses of α-pinene and pinonaldehyde.

Since the time period for early reaction stages for the high-NO condition was slightly adjusted, the previous Figure 2 (now Figure 3) has been updated accordingly. Nevertheless, the overall trends and conclusions remain the same, and no significant differences to the previous version can be observed.

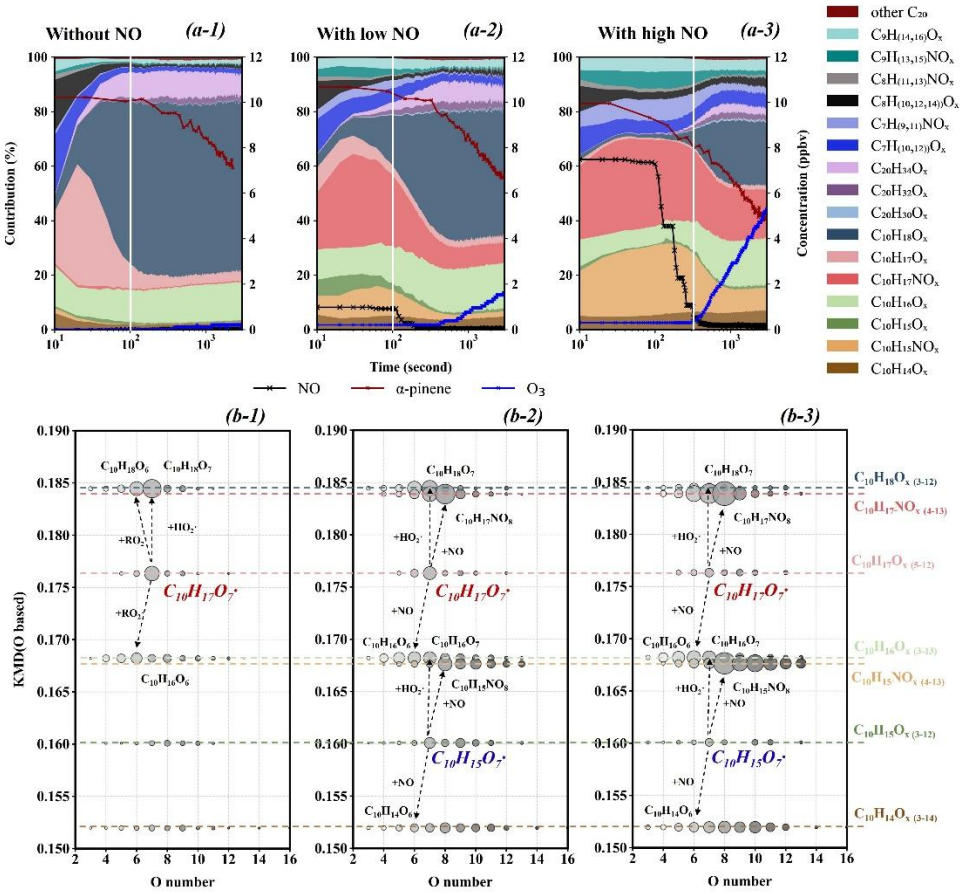

Figure 3. Panels (***a-1, a-2, a-3***) show stacked figures with the contributions of each product family from α-pinene photooxidation as a function of reaction time. The families representing major monomers (C = 10), fragments (C < 10), and accretion products (C = 20) are included in panels ***(a-1, a-2, a-3)***. Time series of concentrations for α-pinene, NO, and O_3 are also presented. The corresponding panels ***(b-1, b-2, b-3)*** located below each stack plot show the Kendrik Mass Defect (KMD, based on oxygen weight) of monomer compounds as a function of oxygen number, with marker sizes indicating the relative abundance of each compound in the early reaction stages (0-100s, 0-100s, and 0-320s after reaction starts for b-1, b-2, and b-3, respectively. This is also indicated by the vertical white lines in a-1, a-2, and a-3). Compounds aligned along the same horizontal dashed lines are in same family, with the same carbon and hydrogen number but differing in oxygen number. Family names are shown on the right. The texts in panels ***(b-1, b-2, b-3)*** highlight major compounds with high abundance and their possible formation pathways. NO conditions increase in the panels from left to right, from NO-free and low-NO to high-NO, respectively. The products here are detected by nitrate-CIMS.

3. A more robust decision could be made by choosing the OH exposure (or reaction time), at which the authors identify a range for "early reaction stage" via some 0D box modeling to quantify pinonaldehyde loss with respect to alpha-pinene loss and relative alpha-pinene loss with respect to O3 oxidation compared to OH oxidation By doing so, the authors will make the discussion in section 3 and statements such as in line 333 ("C10H15O3•, which cannot arise from ozonolysis of α-pinene since O3 formation is negligible in the early reaction stages") more convincing. Finally, because all relevant species are directly measured and calibrated, more quantitative parameters of the RO2 fate could be calculated instead of just estimating the ratio of RO2 reactivity towards NO or HO2.

Responses:

We thank the reviewer for this valuable comment and agree again that model simulations can provide a more quantitative definition of the early reaction stages and strengthen the results. As mentioned before, we have performed additional box-model simulations. The simulations successfully reproduced the observed decay of α-pinene and provided better estimates of the concentrations of the key radicals, including ·OH, RO_2·, and HO_2·.

Using these simulated radical concentrations, we have further evaluated the bimolecular loss pathways of RO_2· radicals, including reactions with HO_2·, NO, and other RO_2· radicals. Details of these calculations are provided in our response to Comment 2.

In addition, we compared the reaction rates of α-pinene with ·OH and O_3 to identify time periods, during which OH-initiated oxidation dominated while O_3-initiated oxidation was negligible. This analysis provides a more quantitative basis for defining the early reaction stages, and supports the results presented in the revised manuscript.

Besides the changes made which have been mentioned in Comment 2, we also revise the discussion part:

The initial peroxy radicals that led to the $C_{10}H_{15}O_x$· related products were identified as $C_{10}H_{15}O_3$·. However, $C_{10}H_{15}O_3$· cannot be the result of ozonolysis of α-pinene since α-pinene was predominantly oxidized by ·OH radicals rather than O_3, as shown in ***Figure S7***.

4. I find discussion used to prove the C10H14Ox compounds come from alpha-pinene H-abstraction instead of pinonaldehyde OH addition unclear. The main issue I have is with the paragraph starting on line 405. First, it is unclear what exactly is being plotted in Figure 4b: the integrated ncps over the course of the experiments or the signal of each species recorded at a similar time. Either way, there is limited discussion on whether [OH]ss or VOC reactivity drives the difference in turnover between alpha-pinene and pinonaldehyde. The loss of closed shell species to OH oxidation could muddle the conclusions here and is not discussed at all. That being said, I think the evidence presented in the paragraph starting at line 429 is the most convincing and robust and should be highlighted more in this discussion and throughout the paper.

Responses:

We thank the reviewer for this valuable suggestion. We agree that normalizing product signals by the pinonaldehyde turnover in each experiment provides a more appropriate basis for evaluating the contribution of pinonaldehyde oxidation to the formation of C10H15Ox-related HOMs observed during α-pinene oxidation. Accordingly, we have made the following revisions:

1. In addition to the previously mentioned box model simulations, we have substantially revised figure 5 (previously Figure 4). The original Figure 4 was intended to compare product distributions between α-pinene and pinonaldehyde experiments, and to assess whether pinonaldehyde oxidation could explain the observed C10H15Ox-related HOMs in α-pinene photooxidation. In the original Figure 4 the pinonaldehyde turnover was not explicitly quantified since we also did not quantify the concentrations of pinonaldehyde. We agree with the reviewer that the description of Figure 4b was insufficient, and that the definition of the "early reaction stage" was not adequately explained and justified. Therefore, we have revised the Figure. The new Figure 5b now presents product distributions averaged over the early reaction stage periods and normalized to the pinonaldehyde turnover ratio between the two experiments.
2. We also appreciate the reviewer's observations that the discussion about the comparison between α-pinene and pinonaldehyde experiments are important and convincing to highlight the importance of H-abstraction chemistry. Therefore, we have expanded the discussion in the manuscript to clarify the normalization procedure and to explicitly account for differences in ·OH exposure and precursor reactivity when evaluating the role of pinonaldehyde oxidation in forming C10H15Ox-related HOMs. We have also emphasized this evidence in both the Abstract and the Conclusions section.

The following text was added to the manuscript, and Figure 5 was updated as shown below:

To assess the potential contribution of pinonaldehyde oxidation to the formation of $C_{10}H_{15}O_x$·-related HOM, pinonaldehyde photooxidation experiments were conducted under NO-free and high-NO conditions,

analogous to conditions applied in the α-pinene systems (***Table 1***). Time series of α-pinene and its oxidation product pinonaldehyde during the first 30 min of the α-pinene (high-NO) experiment are shown in Figure ***5(a-1).*** The corresponding turnovers of α-pinene and pinonaldehyde are presented in Figure ***5(a-1).*** Similarly, the concentration of pinonaldehyde and its turnover during the pinonaldehyde (high-NO) experiment are shown in Figure ***5(a-2).*** ·OH concentrations were estimated using model simulations.

During early stage, the average pinonaldehyde turnover was 8.9×10^6 molecules cm^{-3} s^{-1} under pinonaldehyde (high-NO) condition, approximately 6 times higher than the turnover (1.5×10^6 molecules cm^{-3} s^{-1}) under α-pinene (high-NO) condition. To facilitate comparison between the two experiments, we calculated the pinonaldehyde turnover for both experiments and compared it to obtain the ratio between the high-NO α-pinene and pinonaldehyde experiment (hereafter referred to as the pinonaldehyde turnover ratio). Signals measured in the pinonaldehyde experiment were subsequently normalized by this ratio to account for differences in the pinonaldehyde turnover between the two experimental systems. The distributions of major $C_{10}H_{15}O_x$·-related products observed during the high-NO α-pinene and high-NO pinonaldehyde experiments are presented in Figure 5(b). Major products belonging to the $C_{10}H_{14}O_x$ and $C_{10}H_{15}NO_x$ family detected by both nitrate-CIMS (N) and amine-CIMS (A) are included. The data shown in ***Figure 5(b)*** represents averages over the first 320 s following the initiation of oxidation, corresponding to the early reaction stage, during which RO_2· + NO accounts for more than 90% of the total bimolecular RO_2· loss rate. In addition, all product signals here as well as all data used for comparison in the following paragraphs have been normalized by the pinonaldehyde turnover.

The pinonaldehyde turnover ratio during the first 320 s exceeded 5 and was substantially higher during the first 100 s. This large difference arises because pinonaldehyde was present at the start of the pinonaldehyde high-NO experiment and was therefore immediately available for reaction with ·OH. In contrast, under α-pinene high-NO conditions, pinonaldehyde had to be formed through α-pinene oxidation before it could undergo further reactions, resulting in a much lower pinonaldehyde turnover during the early stages of the experiment. For $C_{10}H_{15}O_x$·-related HOM detected by nitrate-CIMS the summed signals of the $C_{10}H_{14}O_x$ and $C_{10}H_{15}NO_x$ families under α-pinene high-NO conditions exceed those of pinonaldehyde high-NO conditions by factors of approximately 20 and 10, respectively. Although pinonaldehyde oxidation contributes to the formation of $C_{10}H_{15}O_x$·-related HOM under high-NO conditions, this contribution is minor and can explain approximately 5% of the HOM yield observed from α-pinene oxidation. Similarly, for less oxygenated products measured by amine-CIMS, the summed concentrations of the $C_{10}H_{14}O_x$ and $C_{10}H_{15}NO_x$ families were 98 times higher in the α-pinene high-NO experiment, and 6.7 times higher in the pinonaldehyde high-NO experiment.

For highly oxygenated compounds detected by nitrate-CIMS, species containing more than 10 oxygen atoms account for 11% of the $C_{10}H_{14}O_x$ family and for 13% of the $C_{10}H_{15}NO_x$ family under α-pinene

high-NO condition, whereas their contributions are much lower for pinonaldehyde high-NO conditions (3% and 5%, respectively).

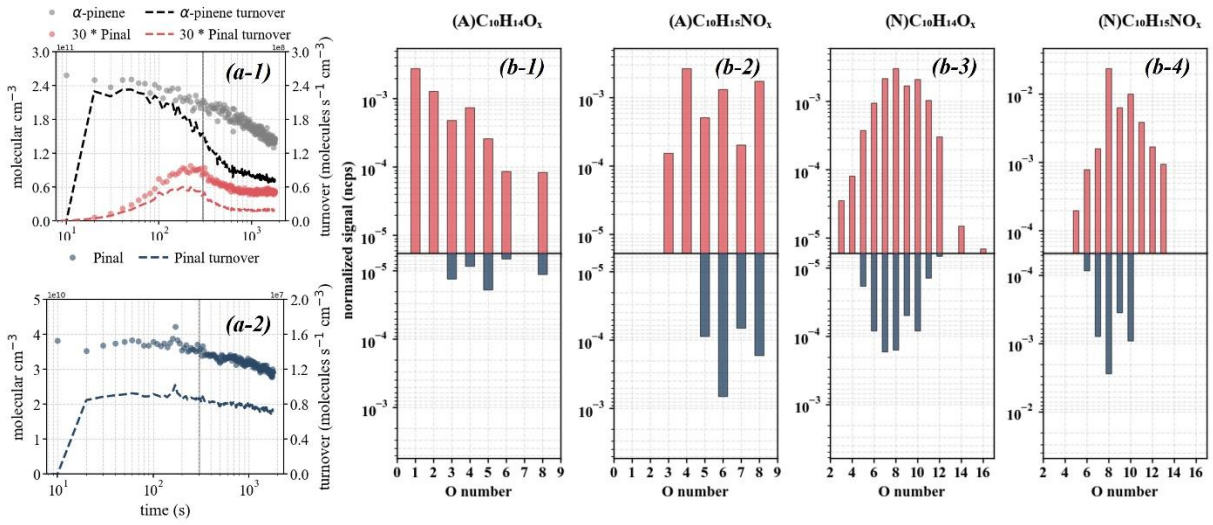

Figure 5. Panel (a-1) displays concentrations and turnover of α-pinene and pinonaldehyde (Pinal) during α-pinene photooxidation under high-NO conditions, while panel (a-2) represents concentrations and turnover of pinonaldehyde during the high-NO pinonaldehyde photooxidation experiment. Major product distributions are shown in panel (b-1) to (b-4). Signals detected in the pinonaldehyde experiment are normalized by the ratio of the pinonaldehyde turnover during the pinonaldehyde experiment to the respective turnover during the α-pinene experiment. The products are separated into four groups: (A)$C_{10}H_{14}O_x$, (A)$C_{10}H_{15}NO_x$, (N)$C_{10}H_{14}O_x$, (N)$C_{10}H_{15}NO_x$, of which (A) and (N) represent signals derived from amine-CIMS and nitrate-CIMS, respectively. Data from α-pinene oxidation and pinonaldehyde oxidation are colored in pink and blue, respectively.

The revised abstract and conclusion are attached below:

Abstract:

Highly oxygenated organic molecules (HOM) are efficiently formed via autooxidation during ·OH-initiated oxidation of α-pinene. We investigated the relative contributions of ·OH-addition and hydrogen (H)-abstraction to HOM formation from α-pinene photooxidation under varying NO conditions. HOM molecules were detected by a nitrate chemical ionization mass spectrometer (CIMS). In the absence of NO, $C_{10}H_{17}O_x$· peroxy radicals and related termination products (e.g. $C_{10}H_{18}O_x$) dominated the HOM spectrum, accounting for more than 70% of total HOM. The presence of NO substantially altered HOM products, particularly by the rapid formation of $C_{10}H_{15}O_x$·-related HOM like $C_{10}H_{15}NO_8$. The ratio of $C_{10}H_{15}NO_x$ to $C_{10}H_{17}NO_x$ increased significantly from 0.34 to 0.84 as the RO_2· loss rate via reaction with NO increased from 0.18 s^{-1} to 1.06 s^{-1}. Under high-NO conditions, $C_{10}H_{15}O_x$·-related HOM contributed up to 34% to total HOM from α-pinene oxidation systems. H-abstraction channel was proven to be the source of $C_{10}H_{15}O_x$·-

related HOM. Fuzzy c-means clustering indicated that $C_{10}H_{15}O_x$·-related HOM exhibited the fastest formation rate among the identified HOM groups, consistent with first-generation products. Comparison with pinonaldehyde oxidation, obtained by normalizing HOM yields to pinonaldehyde turnover, suggests that pinonaldehyde contributed ~5% of HOM in α-pinene systems, excluding secondary oxidation as the dominant source. Detection of $C_{10}H_{15}NO_4$ under high-NO conditions by propylamine-CIMS is indicator for formation of $C_{10}H_{15}O_3$· peroxy radicals, formed by alkoxy radical decomposition and six-membered ring opening in H-abstraction channel. This study highlights the role of the H-abstraction pathway in OH-initiated α-pinene oxidation under NO-influenced conditions and provides new constraints on detailed HOM formation mechanisms.

Conclusion:

To constrain the potential contribution of H-abstraction to HOM formation, regimes with and without NO were directly compared, and a separate experiment of pinonaldehyde oxidation under similar conditions was performed. Additionally, measurements by Amine-CIMS were used to detect less oxygenated products. Since the photolysis of H_2O_2 was utilized to produce ·OH radicals O_3 did not accumulate during the early reaction stages; therefore, ozonolysis did not interfere with the ·OH pathways. FCM analysis proves that the dominant species in the $C_{10}H_{15}NO_x$ family, $C_{10}H_{15}NO_8$ and $C_7H_9NO_8$, can be distinguished from other species by their fast formation rates in the presence of NO. Pinonaldehyde oxidation can only contribute ~ 5% to HOM formation in α-pinene oxidation systems. Therefore, neither ozonolysis nor secondary oxidation can explain the significant formation of $C_{10}H_{15}O_x$·-related HOM, which points to H-abstraction from α-pinene by ·OH being the most likely formation pathway.

As illustrated in ***Figure S12*** and ***Figure S16,*** the contribution of the H-abstraction pathway to HOM formation increases with elevated NO levels compared to the ·OH addition pathway. The ratios between major $C_{10}H_{15}O_x$·-related HOM and $C_{10}H_{17}Ox$·-related HOM rise with increasing NO concentrations. The ratio of $C_{10}H_{15}O_x$· peroxy radicals to $C_{10}H_{17}O_x$· peroxy radicals is 0.06, 0.83, and 1.42 under NO-free, low-NO, and high-NO conditions, respectively. Similarly, the ratio of $C_{10}H_{15}NO_x$ to $C_{10}H_{17}NO_x$ increases from 0.34 to 0.84 when NO levels increase from low to high. The sum of the major $C_{10}H_{15}O_x$·-related closed-shell HOM products ($C_{10}H_{14}O_x$, $C_{10}H_{15}NO_x$ and $C_{10}H_{16}O_x$) contributes 24% and 34% to the total HOM under low-NO and high-NO conditions, while it is negligible under NO-free conditions.

Minor comments

Throughout the figures (Fig 2a, Fig 4a), the NO measurements look stepwise. What was the frequency of data acquisition? Were these points interpolated?

Response:

We thank the reviewer for this comment. The NO monitor acquires a new sample every 45 seconds, which explains the stepwise appearance of the NO in the figures. To compare the NO data with other measurements (e.g., CIMS and PTR data) and model simulations, the NO data was interpolated onto a 10 second grid for consistent temporal alignment. We note that this interpolation does not introduce additional information and only provides a temporally consistent representation for the analysis.

Line 58: It is unclear what is meant by "the latter," as the comparison in the previous paragraph was OH-addition vs OH-abstraction, but C10H17O3• don't form via OH-abstraction.

Response:

We thank the reviewer for mentioning this. We have significantly revised this paragraph to make it clearer:

α-pinene is globally the most abundant monoterpene and has been shown to form significant amounts of HOM when it is oxidized by O_3 or by hydroxyl radical (·OH) (Ehn et al., 2014; Berndt et al., 2016). ·OH initiated oxidation of α-pinene occurs via the OH-addition pathway (~90%) and the hydrogen (H)-abstraction pathway (~10%), leading to the formation of peroxy radicals (RO_2·) with the formulas $C_{10}H_{17}O_3$· and $C_{10}H_{15}O_2$·, respectively (Vereecken et al., 2007).

Line 70: Vereecken et al. (2007) has only a limited discussion of the H-abstraction pathway of alpha-pinene oxidation and only specifically comments on later generation fragmentation products of the H-abstraction pathway in the atmosphere vs the chamber (see figures 3+4).

Response:

We thank the reviewer for this comment. We agree that Vereecken et al. (2007) only provide a limited discussion of the H-abstraction pathway and is not directly appropriate for supporting this statement. We have therefore removed this citation and revised the sentence accordingly:

The detection of $C_{10}H_{15}O_x$ related products with fewer than five oxygen atoms suggests contributions from H-abstraction pathways

Line 181: Grammatical error.

Response:

We thank the reviewer for pointing this error out. We have revised this sentence as follows:

The concentration of ·OH radicals was calculated based on the reacted fraction of α-pinene or pinonaldehyde under steady-state conditions (**Eq.1**) (Kiendler-Scharr et al., 2009). When the system is in steady-state, all parameters are stable and injection rates equal loss rates.

Line 232: "Under no-NO" is formatted awkwardly surrounding the table.

Response:

We thank the reviewer for pointing this error out. We revised this sentence and also changed no-NO to NO-free or "without NO" throughout the manuscript:

Under α-pinene photooxidation conditions without NO, …

Lines 243-249: There is a paragraph break contains multiple ideas. It's a bit hard to follow clearly.

Response:

We thank the reviewer for this comment, and we agree with reviewer that the previous version was difficult to understand. Therefore, we revised this part to:

Compounds with six oxygen atoms but one hydrogen less or one more hydrogen (i.e., $C_{10}H_{16}O_6$ and $C_{10}H_{18}O_6$) are significant contributors to the total product signal of the $C_{10}H_{17}O_x$· family. Compounds with the formula $C_{10}H_{16}O_6$ likely have carbonyl functionalities and are formed either directly from reaction R3 or from self-termination reactions of $C_{10}H_{17}O_7$· (reaction R8) (Iyer et al., 2018; Jenkin et al., 2019). In contrast, $C_{10}H_{18}O_6$ species are possibly alcohols formed from $C_{10}H_{17}O_7$· via reaction R3, or more likely hydroperoxides derived from $C_{10}H_{17}O_6$· via reaction R1 (Iyer et al., 2018; Jenkin et al., 2019).

The following sentence was deleted:

The appearance of compounds with C<10 indicates the formation of alkoxy radicals, since alkoxy radicals can fragment to form species with less than ten carbon atmos.

Line 309: "formula" instead of "formular"

Response:

We that the reviewer for pointing this error out. We replaced formular with 'formula'.

Line 344: Are the KMD plots showing the integrated contribution over the course of the total "early reaction stage" or is it at the top limit?

Response:

We thank the reviewer for this comment. The KMD plots present the average contribution over the entire early-stage reaction period. The related description has been updated:

The average product distributions of C_{10} monomers from early stage α-pinene photooxidation without and with NO are illustrated by Kendrik Mass Defect (KMD) plots as a function of oxygen number (Kendrick Mass = oxygen, ***Figure2 (b-1, b-2, b-3)***).

Line 484: Why would the use of a different type of inlet effect the measurement sensitivity of just one class of HOM? Is there evidence to back up this hypothesis? The experimental conditions and chamber were different between the authors experiments and the Shen et al 2022 experiments. Could that be a reason differences are observed?

Responses:

We thank the reviewer for this comment. We agree that the comparison with Shen et al. (Shen et al., 2022) should be performed with more caution, as the two studies were conducted under different experimental conditions. In the revised manuscript, we have expanded the discussion and now explicitly address several factors that may contribute to the discrepancy, including differences in reaction time, RO_2· fates under high-NO conditions, and instrumental setup.

Although we performed experiments with different ·OH sources, the ·OH level and ·OH exposure are comparable between the two experiments. In our study, more HO_2· radicals were produced due to the reaction between H_2O_2 and ·OH, resulting in an order of magnitude higher HO_2· concentrations compared to Shen et al.'s study (Shen et al., 2022). However, the box model simulations showed that under high-NO conditions the RO_2· + NO reaction rate can explain more than 95% of the biomolecular RO_2· losses, which is consistent with Shen et al. Additionally, only early reaction stages were considered for both studies, during which secondary oxidation was negligible and RO_2· + NO reactions were dominant among RO_2· biomolecular reactions. Therefore, the chemical processes are comparable between the two studies. However, the different chambers could introduce different wall loss rates, which could in turn introduce uncertainty in determining HOM yields and product distributions.

To strengthen the discussion about the different inlets, we now include evidence from a previous inter-comparison measurement designed to evaluate the performance of an Eisele inlet and a MION inlet system. The measurements suggest that the detection efficiency for less-oxygenated HOM (O<8) differs between the two inlet configurations. For example, less-oxygenated C10H17Ox-related HOM were detected with higher efficiency by the MION compared to the Eisele inlet (***Figure S17***). Therefore, the relative

contribution of C10H15Ox-related HOM might be higher in the Eisele inlet. Since this study used a MION inlet, whereas Shen et al. (Shen et al., 2022) used an Eisele inlet, inlet-dependent sensitivity differences could partly explain the lower contribution of H-abstraction related products.

We extended the discussion and added one more plot to show the different measurement results between Eisele inlet and MION inlet (Figure S17):

The contribution of H-abstraction related products observed in this study was lower than that reported by Shen and coworkers, who reported a contribution of more than 70% (Shen et al., 2022). The experiments from the two studies were conducted in different chambers, under different conditions and with different instrumentations applied. Two chambers could introduce different wall losses of HOM, which can be further different between less oxygenated HOM and highly oxygenated HOM.

In this study the ·OH radicals were generated via photolysis of H_2O_2, whereas HONO photolysis was the main source of ·OH in Shen et al. (2022). The consecutive reaction between ·OH and H_2O_2 in our experiments leads to an enhanced production of HO_2· radicals, resulting in an HO_2· concentration of ~4×10^8 molecule cm^{-3}, which is approximately one order of magnitude higher than that reported by Shen et al. (2022). Also, the NO concentration in Shen et al. was constantly around ~20 ppb, while it was only ~7 ppb before reaction in our study, resulting in a concentration of ~1 ppb during the early-reaction stage. Despite these differences, the contributions of RO_2· + NO reactions are dominant in both studies, accounting for more than 95% of RO_2· biomolecular losses under high-NO conditions. In addition, we did only consider early reaction stages, during which secondary oxidation was negligible and RO_2· chemistry was dominated by autoxidation and RO_2· + NO reactions. Therefore, the chemical system can be expected to be similar for both studies, at least under high-NO conditions. However, the constantly higher level of NO in the study by Shen et al. (2022) may continuously promote the H-abstraction channel.

The discrepancy may also arise from differences in measurement techniques: Shen et al. (2022) used an Eisele type inlet (Mauldin et al., 1999), while in this study a MION inlet was used (Rissanen et al., 2019). To compare both inlet systems, we conducted an experiment where both types of inlets were simultaneously used to measure the same oxidation systems. The reference system was α-pinene oxidation by ·OH, with the addition of NO (***Figure S17).*** The results indicate that the MION inlets detects a larger fraction of lesser oxygenated HOM (less than eight oxygen atoms) than the Eisele inlet, and that these HOM dominate the $C_{10}H_{17}O_x$·-related HOM family, while the relative contribution of higher oxygenated HOM (more than eight oxygen atoms) was larger in the study by Shen et al. (2022). When only the highly oxygenated HOM compounds are considered as was done in the study be Shen and coworkers, the relative contribution of $C_{10}H_{15}O_x$·-related HOM to the total HOM does increase to 64%. Therefore, a deeper comparison of the two inlet types may be of interest in the future but is outside the scope of this study.

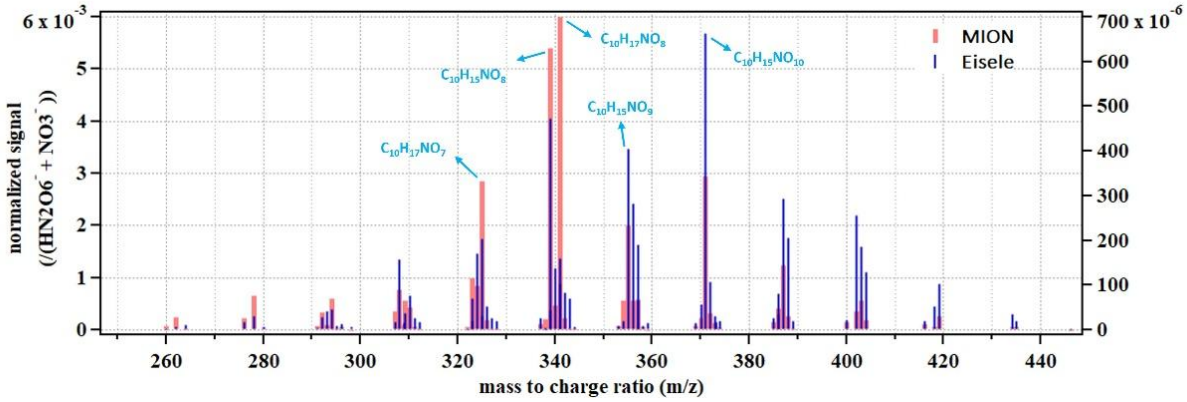

Figure S17. The signal of products derived from α-pinene oxidation with NO injection, detected by CIMS coupled with the MION (pink) and Eisele (blue) inlets.

References:

Baker, Y., Kang, S., Wang, H., Wu, R., Xu, J., Zanders, A., He, Q., Hohaus, T., Ziehm, T., Geretti, V., Bannan, T. J., O'Meara, S. P., Voliotis, A., Hallquist, M., McFiggans, G., Zorn, S. R., Wahner, A., and Mentel, T. F.: Impact of HO2/RO2 ratio on highly oxygenated α-pinene photooxidation products and secondary organic aerosol formation potential, Atmos. Chem. Phys., 24, 4789-4807, 10.5194/acp-24-4789-2024, 2024.

Berndt, T., Richters, S., Jokinen, T., Hyttinen, N., Kurten, T., Otkjaer, R. V., Kjaergaard, H. G., Stratmann, F., Herrmann, H., Sipila, M., Kulmala, M., and Ehn, M.: Hydroxyl radical-induced formation of highly oxidized organic compounds, NATURE COMMUNICATIONS, 7, 10.1038/ncomms13677, 2016.

Iyer, S., Reiman, H., Moller, K. H., Rissanen, M. P., Kjaergaard, H. G., and Kurten, T.: Computational Investigation of RO(2) + HO(2) and RO(2) + RO(2) Reactions of Monoterpene Derived First-Generation Peroxy Radicals Leading to Radical Recycling, J Phys Chem A, 122, 9542-9552, 10.1021/acs.jpca.8b09241, 2018.

Jenkin, M. E., Saunders, S. M., and Pilling, M. J.: The tropospheric degradation of volatile organic compounds: a protocol for mechanism development, Atmospheric Environment, 31, 81-104, https://doi.org/10.1016/S1352-2310(96)00105-7, 1997.

Jenkin, M. E., Valorso, R., Aumont, B., and Rickard, A. R.: Estimation of rate coefficients and branching ratios for reactions of organic peroxy radicals for use in automated mechanism construction, Atmospheric Chemistry and Physics, 19, 7691-7717, 10.5194/acp-19-7691-2019, 2019.

Kiendler-Scharr, A., Wildt, J., Dal Maso, M., Hohaus, T., Kleist, E., Mentel, T. F., Tillmann, R., Uerlings, R., Schurr, U., and Wahner, A.: New particle formation in forests inhibited by isoprene emissions, Nature, 461, 381-384, 10.1038/nature08292, 2009.

Mauldin, R. L., Tanner, D. J., Heath, J. A., Huebert, B. J., and Eisele, F. L.: Observations of H2SO4and MSA during PEM-Tropics-A, Journal of Geophysical Research: Atmospheres, 104, 5801-5816, 10.1029/98jd02612, 1999.

Saunders, S. M.; Jenkin, M. E.; Derwent, R. G.; Pilling, M. J.: Protocol for the development of the Master Chemical Mechanism, MCM v3 (Part A): tropospheric degradation of non-aromatic volatile organic compounds. Atmos. Chem. Phys. 2003, *3* (1), 161-180. DOI: 10.5194/acp-3-161-2003.

Shen, H., Vereecken, L., Kang, S., Pullinen, I., Fuchs, H., Zhao, D., and Mentel, T. F.: Unexpected significance of a minor reaction pathway in daytime formation of biogenic highly oxygenated organic compounds, Science Advances, 8, eabp8702, doi:10.1126/sciadv.abp8702, 2022.

Vereecken, L., Muller, J. F., and Peeters, J.: Low-volatility poly-oxygenates in the OH-initiated atmospheric oxidation of alpha-pinene: impact of non-traditional peroxyl radical chemistry, Phys Chem Chem Phys, 9, 5241-5248, 10.1039/b708023a, 2007

Wu, R., Zorn, S. R., Kang, S., Kiendler-Scharr, A., Wahner, A., and Mentel, T. F.: Application of fuzzy c-means clustering for analysis of chemical ionization mass spectra: insights into the gas phase chemistry of NO3-initiated oxidation of isoprene, Atmospheric Measurement Techniques, 17, 1811-1835, 10.5194/amt-17-1811-2024, 2024.

Yan, C., Nie, W., Äijälä, M., Rissanen, M. P., Canagaratna, M. R., Massoli, P., Junninen, H., Jokinen, T., Sarnela, N., Häme, S. A. K., Schobesberger, S., Canonaco, F., Yao, L., Prévôt, A. S. H., Petäjä, T., Kulmala, M., Sipilä, M., Worsnop, D. R., and Ehn, M.: Source characterization of highly oxidized multifunctional compounds in a boreal forest environment using positive matrix factorization, Atmospheric Chemistry and Physics, 16, 12715-12731, 10.5194/acp-16-12715-2016, 2016.

Zhang, J., Zhao, J., Luo, Y., Mickwitz, V., Worsnop, D., and Ehn, M.: On the potential use of highly oxygenated organic molecules (HOMs) as indicators for ozone formation sensitivity, Atmospheric Chemistry and Physics, 24, 2885-2911, 10.5194/acp-24-2885-2024, 2024.